Supporting Materials to

Differential Mechanical Stability of Filamin A Rod Segments

Hu Chen,[†] Xiaoying Zhu,[‡] Peiwen Cong,[§] Michael P. Sheetz,[†,¶] Fumihiko Nakamura,[‖] and Jie Yan[†,‡,**,*]

[†]Mechanobiology Institute, National University of Singapore, Singapore;
[‡]Department of Physics, National University of Singapore, Singapore;
[§]Singapore-MIT Alliance, National University of Singapore, Singapore;
[¶]Department of Biological Sciences, Columbia University, New York, NY, USA;
[‖]Translational Medicine Division, Department of Medicine, Brigham and Women's Hospital, Harvard Medical School, Boston, MA, USA;
[**]Centre for Bioimaging Sciences, National University of Singapore, Singapore.

Preparation of protein constructs

IgFLNa1-8 was expressed with N-terminal hexahistidine (His) tag and C-terminal Avi-tag as previously described (2). The IgFLNa8-15 and IgFLNa16-23 with N-terminal His-tag and C-terminal Avi-tag were engineered as follows.

The cDNA encoding IgFLNa8-15 was amplified by PCR from cDNA of human FLNa with 5' primer having an EcoRI site GGAATTCCTGGACCTCAGCAAGATC and 3' primer having an NheI site CTAGCTAGCCGTCACTTGGAAGGGGC, and inserted into pFASTBAC-HTa-AviTag digested with EcoRI/XbaI.

The cDNA encoding IgFLNa16-23 was amplified by PCR with 5' primer having a SpeI site GACTAGTGCCCCGGAGAGGCCCCTG and 3' primer having a XbaI site GCTCTAGAGACGAGACGGGGGCCTGTG, and inserted into pFASTBAC-HTb-AviTag digested with XbaI and alkaline phosphatase to generate pFASTBAC-HTb-IgFLNa16-23-AviTag. Fusion proteins were expressed in Sf9 cells, purified, and biotinylated as previously described (2).

Magnetic tweezers

Vertical magnetic tweezers was built based on inverted microscope Olympus IX71. Oil immersion objective UPlanFLN from Olympus with 100X magnification and Numerical Aperture 1.3 was used to image beads. A piezo objective actuator F100 (Madcitylab, USA) was used to move the objective vertically to change its focal plane with high speed and accuracy. Two magnetic rods were placed without gap in between to generate high force (3). A half/half mirror was used to reflect light from Halogen lamp to illuminate the sample through the objective. A Pike F-032B camera (Allied Vision Technologies, Germany) was used to capture images of the bead. An MP285 manipulator (Sutter Instrument Company, USA) or linear stage VT-40 (Micos, Germany) was used to move the magnets to control the force.

Analysis of bead images gives space resolution of ~2 nm in all three dimensions (4). The force calibration was described in our previous paper (2).

Authors (Hu Chen and Xiaoying Zhu) contributed equally to this work.
* Correspondence: phyyj@nus.edu.sg

Force-clamp control: We keep the magnets at fixed position, so constant force is applied to the tether. After 30 seconds, we move the magnets 0.5 mm closer to the sample to apply a bigger force, and hold the constant force for 30 seconds too, until magnets touch the sample.

Loading rate control: With known function of $F(d)$, we designed a trajectory of $d(t)$ to make $F(t)=F(d(t))$ a linear function with pre-defined loading rate as the slope.

Sample preparation

Coverslips were cleaned and functionalized following similar protocol in (5). No. 1.5 Coverslips were washed by detergent and rinsed by DI water. Then they were incubated in 10% H_2O_2, 90% H_2SO_4 for 10 minutes. DI water and 1 M NaOH were used to wash the coverslips. After washing, the coverslips were heated for 60 minutes at 100 ^oC. Then immediately 94% ethanol, 5% H2O, and 1% 3-aminopropyltriethoxysilane (APTES, A3648, Sigma) was applied and incubated for 1 minutes. The coverslips were washed 3 times by ethanol, heated for 10 minutes at 100°C to eliminate ethanol and dry the coverslips.

Channels were made by sandwiching the APTES functionalized No. 1.5 coverslip and No. 0 coverslip with parafilm in between. Parafilm was sealed by gentle heating (Fig. S1). Thin channel is critical to make permanent magnets as close as possible to bottom surface of channel to get high force.

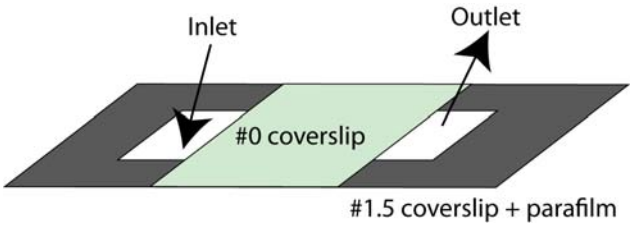

Figure S1: Sketch of sample channel sandwiched by functionalized #1.5 coverslip, parafilm, and #0 coverslip. Inlet and Outlet were used to flow in/out sample.

Then 0.1% glutaraldehyde (G-7526, Sigma) in DI water was incubated in channel for 1 hour, and DI water was used to wash the channel. 1 ug/ml N_α,N_α-Bis(carboxymethyl)-L-lysine hydrate (14580, sigma) in DI water was incubated for 1 hour, then DI water was used to wash the channel. 3-um polybead Amino Microsphere (Polysciences, Inc) was cleaned and diluted around 200X in DI water, then flowed into the channel and incubated for 20 minutes. These beads are fixed onto the surface and they serve as reference to eliminate drift. After this step, channel was washed by Tris buffer with pH 8. Then 100 mM nickel sulfate or copper sulfate was flowed in channel. 1% BSA solution was used to block the surface overnight.

Finally, around 1 nM IgFLNa 1-8, IgFLNa 8-15, or IgFLNa 16-23 in buffer containing 20 mM Tris pH 8, 300 mM NaCl, 2 mM $MgCl_2$, 1 mM 2-Mercaptoethanol, and 1% BSA was incubated in channel for 20 minutes. Then streptavidin-coated paramagnetic bead (dynal M-280, Invitrogen, Inc) was flowed into the channel. After incubation for 20 minutes, unattached beads were washed away using the same buffer. Mineral oil was applied at the inlet and outlet of channel to avoid evaporation.

The specificity of the tethers was checked in experiments. When the surface was not incubated with proteins or when it was incubated with proteins unlabelled with biotin, the probability of

finding streptavidin-coated beads bound to the surface is at least 10 times less than when the surface was incubated with biotinylated proteins. In addition, those rare non-specific tethers did not give the characteristic stepwise unfolding signals.

Signal from multi-tether vs. single-tether

When there are more than one protein tethers between paramagnetic bead and coverslip surface, the unfolding signal is different from single tether. When two or more tethers form between the bead and the surface, simultaneous unfolding of domains from all tethers is unlikely. When a domain in a tether unfolds and lengthens, the torque applied on the bead will not be balanced. This will cause bead rotations, and as a result, the bead position in the focal plane will change synchronized with the change in extension along the force direction. A typical example is shown in the left panel of Fig. S2. In contrast, when a single tether is stretched, unfolding only causes extension increase along the force direction (right panel, Fig. S2). One advantage of magnetic tweezers over AFM is that three-dimensional location of bead can be monitored, while AFM only measure the extension.

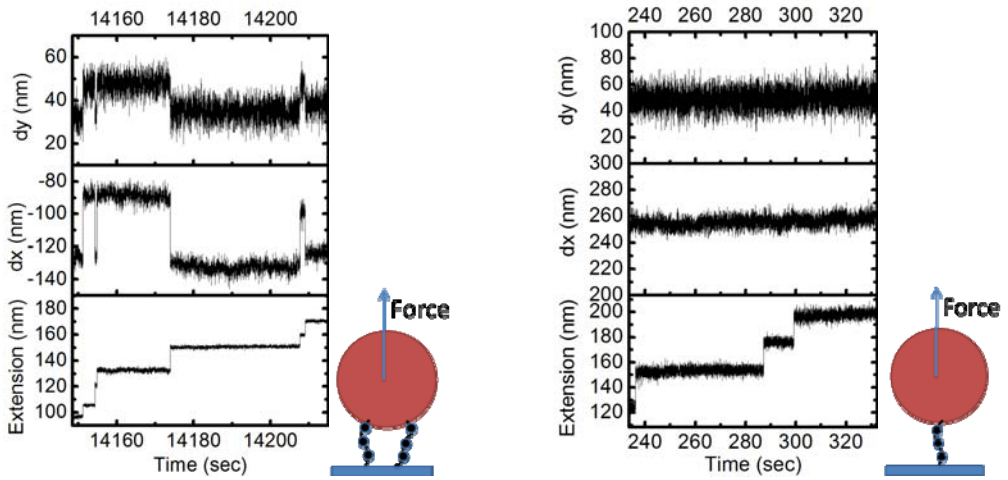

Figure S2: Typical signal of multi-tether (left panel) and single tether (right panel). For multi-tether, when unfolding event occurs, the extension increases stepwisely. At the same time, location of the tethered bead in focal plane dx and dy jump too, which indicates the rotation of the bead due to un-balanced torque. While for single tether, dx, dy keep at constant values when protein unfolds.

Distributions of unfolding forces of IgFLNa 1-8 under different loading rates

Protein unfolding needs to cross over an energy barrier, thus it is a stochastic process. Due to the energy barrier, the unfolding force depends on the loading rate. Generally, with higher loading rate, the protein has less time to cross over the energy barrier. Therefore, the unfolding tends to occur at higher forces. Fig. S3 shows the histogram of unfolding forces for IgFLNa 1-8 at three different loading rates ~0.16 pN/sec, ~1.6 pN/sec, and ~16 pN/sec.

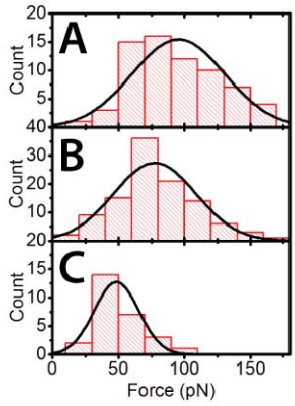

Figure S3: Unfolding force distribution of IgFLNa 1-8 under loading rate of ~16 pN/second (A), ~1.6 pN/second (B), and ~0.16 pN/second (C). Black solid curves are Gaussian fitting of the distribution.

Stretching geometry

The mechanical stability of protein is dependent on pulling geometry. In general, two β-strands can withstand a higher rupture force in shearing force geometry than in unzipping force geometry (see sketch in Fig. S4). A well-known example is the rupture of the two DNA strands in double-stranded DNA (note: they are not β-strands, but they are associated with hydrogen bonds, so the physical principle is the same): the rupture force is ~15 pN (6) in the unzipping geometry, while it is ~60 pN in the shearing geometry (7). The main reason is that in the unzipping geometry, breaking one bond leads to a greater extension change along the force direction than in the shearing geometry.

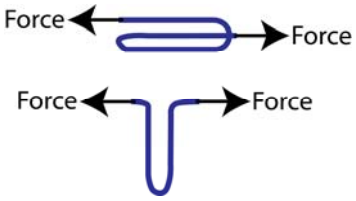

Figure S4: Simplified schematic figure of the pulling geometries of shearing force (upper panel) and unzipping force (bottom panel). Individual Immunoglobulin (Ig) domains with seven beta strands are stretched by shearing force, while the domain pairs IgFLNa18-19 and 20-21 are stretched by unzipping force.

Loading rate estimate in AFM experiment

In AFM experiment, protein end is pulled by constant speed of 0.37 um/second. The loading rate is not constant.

According to Worm-Like Chain (WLC) model, the relationship between force F and extension x is given by equation:

$$\frac{FA}{k_B T} = \frac{1}{4}\left(1 - x/L\right)^{-2} - \frac{1}{4} + x/L$$,

where A is persistence length, k_B is Boltzmann's constant, T is absolute temperature, and L is the contour length. The loading rate can be derived as:

$$\frac{dF}{dt} = \frac{k_B T}{AL}\left[\frac{1}{2}\left(1 - x/L\right)^{-3} + 1\right]\frac{dx}{dt}$$.

When we set parameters F=150 pN which is the typical unfolding force in (1), A=0.33 nm which was fitted in the AFM experiments, x/L = 0.856 is determined. If we set L=300 nm which is close to the average contour length observed in (1), and with known pulling rate of 370 nm/seond, we estimated a loading rate dF/dt ~2500 pN/second for the AFM experiments. Even when we set unfolding force F=50 pN, the loading rate is still ~500 pN/second. They are much larger than the magnetic tweezers experiment with loading rate ~1.6 pN/second.

Overall distribution of unfolded contour length

To compare the contour length distribution of our magnetic tweezers results with previous AFM experiment of pulling full-length FLNa (1) we plot both results together in Fig. S5 (the AFM data were reproduced from Fig. 2 (b) from reference (1)). The two distributions agree with each other reasonably well. We observed more number of small unfolding steps than AFM. The possible reason is that we pull the protein with much lower loading rate, so we have higher chance to observe intermediate state of unfolding.

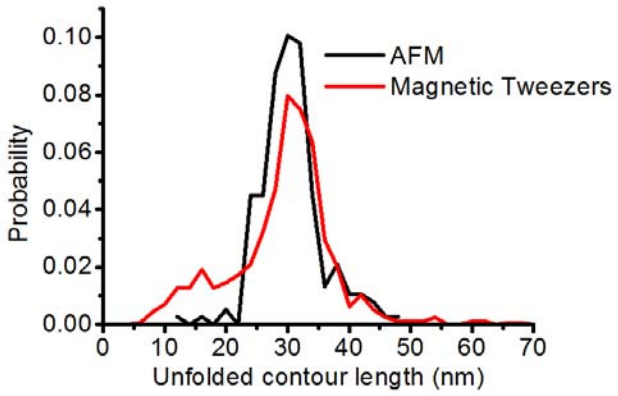

Figure S5: Probability of unfolded contour length. AFM data are from (1), and Magnetic Tweezers results are from all experiment of IgFLNa 1-8, 8-15, and 16-23.

References

1. Furuike, S., T. Ito, and M. Yamazaki. 2001. Mechanical unfolding of single filamin A (ABP-280) molecules detected by atomic force microscopy. FEBS Lett 498:72-75.

2. Chen, H., H. Fu, X. Zhu, P. Cong, F. Nakamura, and J. Yan. 2011. Improved high-force magnetic tweezers for stretching and refolding of proteins and short DNA. Biophys J 100:517-523.

3. Lipfert, J., X. Hao, and N. H. Dekker. 2009. Quantitative modeling and optimization of magnetic tweezers. Biophys J 96:5040-5049.

4. Gosse, C., and V. Croquette. 2002. Magnetic tweezers: micromanipulation and force measurement at the molecular level. Biophys J 82:3314-3329.

5. Delanoe-Ayari, H., R. Al Kurdi, M. Vallade, D. Gulino-Debrac, and D. Riveline. 2004. Membrane and acto-myosin tension promote clustering of adhesion proteins. Proc Natl Acad Sci U S A 101:2229-2234.

6. Bockelmann, U., B. EssevazRoulet, and F. Heslot. 1997. Molecular stick-slip motion revealed by opening DNA with piconewton forces. Phys. Rev. Lett. 79:4489-4492.

7. Smith, S. B., Y. Cui, and C. Bustamante. 1996. Overstretching B-DNA: the elastic response of individual double-stranded and single-stranded DNA molecules. Science 271:795-799.